Dynamic mean-field and cavity methods for diluted Ising systems

Erik Aurell[1,2,3] and Hamed Mahmoudi[2]
[1]*Department of Computational Biology, AlbaNova University Centre, 106 91 Stockholm, Sweden*
[2]*Department of Information and Computer Science, Aalto University, Finland*
[3]*ACCESS Linnaeus Centre, KTH–Royal Institute of Technology, Stockholm, Sweden*
(Received 22 September 2011; published 16 March 2012)

We compare dynamic mean-field and dynamic cavity methods to describe the stationary states of dilute kinetic Ising models. We compute dynamic mean-field theory by expanding in interaction strength to third order, and we compare to the exact dynamic mean-field theory for fully asymmetric networks. We show that in diluted networks, the dynamic cavity method generally predicts magnetizations of individual spins better than both first-order ("naive") and second-order ("TAP") dynamic mean-field theory.

DOI: 10.1103/PhysRevE.85.031119 PACS number(s): 64.60.−i, 68.43.De, 75.10.Nr, 24.10.Ht

I. INTRODUCTION

(Classical) statistical mechanical systems in equilibrium are described by the Gibbs measure, which connects the propensity of a system to move between two states taken in isolation (the energy differences between these two states) to the probability of finding the system in one of the states, when all states are available. This relation is normally used to find equilibrium statistics of a system (magnetizations, correlation functions, etc.) by sampling a dynamics for which the Gibbs measure is a stationary state. A Markov chain Monte Carlo (MCMC) method, such as Glauber dynamics for Ising systems, which we will review briefly below in Sec. II, can work if the sample average converges quickly enough to Gibbs measure, and if the quantity to be measured has wide support in phase space. Well-known scenarios in which this is the case are spin systems in the high-temperature phase and when measuring, e.g., total magnetization. In the low-temperature phase, the relaxation time to the Gibbs distribution can be very long. On the other hand, if the quantity to be measured is, e.g., the magnetization of a single spin, then MCMC in a large system is slow for the trivial reason that one needs to sweep through all the spins while just being interested in the changes in and the average over one of them. If the interactions are weak, marginal probability distributions can be computed perturbatively in mean-field theory [1–3], which give closed equations for, e.g., single-spin magnetizations. For dilute systems, where every spin is not connected to most other spins, very powerful *message-passing* methods have been developed by physicists, information theorists, and computer scientists over the past two decades to compute marginals of Gibbs distributions quickly and accurately [4,5]. While these *cavity equations* cannot (in their simplest form) deal with the complex phases of random spin systems at low temperature, in suitable scenarios they are much more accurate than mean-field theory, and they greatly improve on MCMC for single-site magnetization and other local properties by substituting a cumbersome sampling by a direct deterministic computation. The cavity method has been found to have many technological as well as fundamental applications [5–9].

The situation is very different for out-of-equilibrium systems, which in itself is an extremely broad term covering everything from macroscopic hydrodynamics (turbulence) [10] and physical and chemical kinetics [11] to interdisciplinary applications of statistical physics to neuroscience, population biology, and other fields [12,13]. We consider here the model systems obtained when generalizing the MCMC rules of Ising spin systems (Glauber dynamics) from the equilibrium case (symmetric interactions) to a nonequilibrium case (nonsymmetric interactions). Such "kinetic Ising" models are only conceptual—but tractable—models of real spin systems driven out of equilibrium, and have mainly been studied with applications to neuroscience in mind [14–17]. From a mathematical point of view, they are specific examples of Markov chains that do not obey detailed balance conditions. In contrast to equilibrium systems, there is hence no simple expression for a stationary state akin to a Gibbs measure, but such a state, when it exists, is a (complicated) function of all the details of the model. On the other hand, MCMC works as well in such systems as for standard equilibrium Ising models, and mean-field theory has been developed up to second order in the interaction strength [18]. This leaves open the case of dilute kinetic Ising models, where in the equilibrium case cavity methods would be preferable. A dynamic cavity method has only very recently been developed for majority dynamics [19] and Glauber dynamics [20] and was investigated by us for parallel and sequential update schemes in [21].

The dynamic cavity method as outlined in [21] comprises first an ansatz on probability distributions, similar to a standard cavity, then the belief propagation (BP) ansatz that cavity distributions factorize, and then also a further assumption of Markovianity. As discussed in [22], the second assumption is exact for fully asymmetric models with the parallel update rule. In a more general case, however, in which either the interaction matrix has both a symmetric and an asymmetric component or the update rule is different, it is merely an approximation. The numerical results of [21], which showed that for some such mixed instances the dynamic cavity is quite accurate, were somewhat unexpected. The main motivation for the present paper is therefore to show more systematically in what parameter ranges the dynamic cavity converges (for these models), where it is accurate compared to MCMC, and to compare its predictions to mean-field theory. We will show that for dilute kinetic Ising models, the dynamic cavity works also for the magnetizations of individual spins, and is

considerably more accurate than mean-field calculations of the same quantities.

Kinetic Ising models have been studied with other approaches, and we outline them briefly here. When the discreteness of states is relaxed to a spherical Ising model, Sompolinsky and Zippelius developed a Langevin equation formalism [23], later extended by Crisanti and Sompolinsky to the nonequilibrium case [24], where several phases of these (dynamical) models are outlined. Although pioneering, predicting magnetizations of individual spins is beyond the scope of such methods, as the sphericity approximation has been made. The dynamic replica theory (DRT) has been applied to kinetic Ising models [25]. However, due to the nature of replica theory, it only applies to averages over ensembles of models. Sommers developed a path-integral formulation for the Glauber dynamics [26], which was at that time only investigated approximately. As an alternative approach to path-integral formulation, generating functional analysis was developed to study nonequilibrium statistical mechanics of disordered systems [27]. It was shown by Neri and Bollé in [20] that at least in some cases, a dynamic cavity analysis explicitly averaged over a random ensemble recovers the results of generating functional analysis. Recently, Hertz and Roudi [28,29] used generating functional analysis to derive mean-field theories for infinite-range spin glass models. Another motivation for this work was to compare the accuracy of the predictions of single-site magnetizations by the dynamic mean-field formula of [28] to the dynamic cavity for dilute mixed models.

The paper is organized as follows. In Sec. II, we describe the Glauber dynamics for spin glasses, the model that we will study. In Sec. III, we discuss two approaches to a dynamic version of the TAP corrections to first-order mean-field theory [18,28–30], while in Sec. IV we derive dynamic cavity equations for diluted networks in parallel update. This derivation should be seen as a clearer alternative (we hope) to [20] and our earlier contribution [21]. The main results of this paper, on the convergence phase of the dynamic cavity and on a comparison between the predictions of dynamic cavity and mean-field theory to MCMC, are presented in Sec. V. In Sec. VI, we conclude and discuss possible application areas of the dynamic cavity.

II. THE PARALLEL SPIN UPDATE SCHEME IN DILUTE KINETIC ISING MODELS

The asymmetric dilute Ising model is defined over a set of N binary variables $\vec{\sigma} = \{\sigma_1, \ldots, \sigma_N\}$, and an asymmetric graph $G = (V, E)$, where V is a set of N vertices and E is a set of directed edges. A binary variable σ_i is associated with each vertex v_i. The graphs G are taken from random graph ensembles with bounded average connectivity. Following the parametrization of [27], we introduce a connectivity matrix c_{ij}, where $c_{ij} = 1$ if there is a link from vertex i to vertex j, $c_{ij} = 0$ otherwise, and matrix elements c_{ij} and c_{kl} are independent unless $\{kl\} = \{ji\}$. The random graph is then specified by marginal (one-link) distributions

$$p(c_{ij}) = \frac{c}{N}\delta_{1,c_{ij}} + \left(1 - \frac{c}{N}\right)\delta_{0,c_{ij}} \tag{1}$$

and conditional distributions

$$p(c_{ij} \mid c_{ji}) = \epsilon\delta_{c_{ij},c_{ji}} + (1-\epsilon)\, p(c_{ij}), \tag{2}$$

where $i, j \in \{1, \ldots, N\}$ and $i < j$. In this model, the average degree distribution is given by c, and the asymmetry is controlled by $\epsilon \in [0,1]$. The two extreme values of ϵ give, respectively, a fully asymmetric network ($\epsilon = 0$), where the probabilities of having two directed links between pairs of variables are uncorrelated, and a symmetric network ($\epsilon = 1$), where the two links $i \to j$ and $j \to i$ are present or absent together. The parameter set is completed by a (real-valued) interaction matrix J_{ij}. Additional assumptions on the J_{ij}, i.e., smallness or that they are random with suitable distribution, are stated when used. However, for concreteness, the reader may in much of this paper think of J_{ij} as being independent identically distributed random variables with zero mean and variance $\frac{1}{c}$ (Gaussian or binary) such that for the fully connected networks ($c = N$), the interactions scale as the Sherrington-Kirkpatrick model [31].

The interactions among spins determine the dynamics of the system. In the parallel update scheme, which will be considered here, at each (discrete) time, all spins are updated according to the Glauber rule,

$$\sigma_i(t+1) = \begin{cases} +1 & \text{with probability } \{1 + \exp[-2\beta\, h_i(t+1)]\}^{-1}, \\ -1 & \text{with probability } \{1 + \exp[2\beta\, h_i(t+1)]\}^{-1}, \end{cases} \tag{3}$$

where $h_i(t)$ is the effective field acting on spin i at time step t,

$$h_i(t) = \sum_{j \in \partial i} J_{ji}\, \sigma_j(t-1) + \theta_i(t), \tag{4}$$

and the parameter β, analogous to inverse temperature, is a measure of the overall strength of the interactions. The notation $j \in \partial i$ in (3) and (4) indicates all vertices having a direct link to node i and θ_i is the (possibly time-dependent) external field acting on spin i. In this paper, we will adhere to the convention that the interaction indices are written in the same order as the temporal order of the interacting spins. Hence we have $J_{ij}\sigma_i(s)\sigma_j(s+1)$ and $J_{ji}\sigma_j(s)\sigma_i(s+1)$.

The joint probability distribution over all the spin histories $p(\vec{\sigma}(0), \ldots, \vec{\sigma}(t))$ has in principle the following simple Markov form:

$$P(\vec{\sigma}(0), \ldots, \vec{\sigma}(t)) = \prod_{s=1}^{t} W[\,\vec{\sigma}(s) \mid \vec{h}(s)]\; p(\vec{\sigma}(0)), \tag{5}$$

where W is the appropriate transition matrix describing dynamics and updates. If we had a full understanding of joint probability distribution defined in (5), we could compute time-dependent macroscopic quantities such as magnetization and correlations. The evolution of a single spin is (trivially) defined by summing over the histories of all spins except one,

$$P_i(\sigma_i(0), \ldots, \sigma_i(t)) = \sum_{\vec{\sigma}_{\setminus i}(0), \ldots, \vec{\sigma}_{\setminus i}(t)} P(\vec{\sigma}(0), \ldots, \vec{\sigma}(t)), \tag{6}$$

which can be further marginalized to the probability of one spin at one time,

$$p_i[\sigma_i(s)] = \sum_{\sigma_i(0),\ldots,\sigma_i(s-1),\sigma_i(s+1),\ldots,\sigma_i(t)} P_i(\sigma_i(0),\ldots,\sigma_i(t)), \tag{7}$$

and similarly for pairwise joint probability of the histories of two spins, $P_{ij}(\sigma_i(0),\ldots\sigma_i(t),\sigma_j(0),\ldots,\sigma_j(t))$ and $p_{ij}(\sigma_i(s),\sigma_j(s'))$. Consequently, the time evolution of single-site magnetization can be obtained from Eq. (6) as

$$m_i(t) = \sum_{\sigma_i(t)} \sigma_i(t)\, p_i[\sigma_i(t)] \tag{8}$$

and similarly the correlation functions

$$c_{ij}(s,t) = \sum_{\sigma_i(s),\sigma_j(t)} \sigma_i(s)\sigma_j(t) p_{ij}(\sigma_i(s),\sigma_j(t)). \tag{9}$$

Substituting Eq. (8) into the dynamics defined in (5), we have

$$m_i(t) = \left\langle \tanh\left(\sum_{j\in\partial i} J_{ji}\sigma_j(t-1) + \theta_i(t) \right) \right\rangle, \tag{10}$$

where the angular brackets are the average with respect to trajectory history. Equation (10) is exact for the time-dependent magnetization. It is not directly practical, since the marginal over one spin at one time (the magnetization) depends on the joint distribution of all the spins influencing it at the previous time, but as we will see in Sec. III B, it can be used as a starting point of a perturbative calculation.

III. MEAN-FIELD THEORIES, TAP, AND THE EXPANSION IN SMALL INTERACTIONS

The mean-field theory of spin glass systems started with the Sherrington-Kirkpatrick (SK) model [31]. In this model, all spins interact with all other spins (infinite-range couplings), which motivates the simplest mean-field or "naive mean-field" approximation $m_i = \tanh\beta(\sum_j J_{ji}m_j + \theta_i)$. Shortly afterward, a more accurate mean-field theory (TAP) was introduced by introducing the Onsager reaction for the SK model. This corrects m_j inside the tanh to $m_j - \beta J_{ij}m_i(1-m_j)^2$, where $J_{ij}m_i$ is the field from spin i on spin j and where $\chi_{jj} = \beta(1-m_j^2)$ can be interpreted as a local susceptibility at spin j [1]. Since in equilibrium the Ising $J_{ij} = J_{ji}$, the TAP equilibrium mean-field theory is hence $m_i = \tanh(\beta\sum_j J_{ji}m_j + \beta\theta_i - \beta^2 m_i \sum_j J_{ji}^2(1-m_j^2))$. As stated in [1], these results can be derived from the cavity approach. These can also be derived by observing that in equilibrium, a susceptibility is related to a correlation by fluctuation dissipation, and the appropriate correlation was computed by a perturbative argument [1]. For a later approach using field-theoretical methods, expanding a functional determinant describing the fluctuations around a mean-field stationary point of an action, see, e.g., [32] and references therein.

In equilibrium Ising systems, the naive mean-field and the TAP approximations can further be computed by expanding the Boltzmann distribution in the interaction strength [33]. To first and second order in interactions, this result agrees with naive mean-field and TAP.

Recently, a dynamic version of TAP was derived by Hertz and Roudi [28,29] by a field-theoretical argument, and we show here in Sec. III B below that this also follows from information geometry, essentially a systematic expansion in interaction strength. For completeness, we will also show that the same dynamic version of TAP follows from the "exact mean-field theory" of Mézard and Sakellariou [30], as already pointed out in [34].

Outside equilibrium fluctuation dissipation does not hold. Conceptually one could therefore say that "dynamic TAP" as such is undefined, or, alternatively, that a proper generalization of TAP to a nonequilibrium system should be based on fluctuation relations generalizing fluctuation-dissipation theorems [35] (a task we have not attempted to carry out). In this paper, however, we take a more pragmatic approach, and understand "dynamic TAP" to be the formulas derived in [28,29].

Before turning to the technical discussion, let us note that since mean-field and TAP have obvious computational advantages, these theories have been applied in much wider settings than those in which they have been derived, particularly in neuroscience. For a recent review, see [36] and references therein.

A. Fully asymmetric networks: A reduced theory

In this subsection, we recall the theory in [30], with a view to compute the expansion in small interactions to third order. We start by rewriting the exact equation (10) in the following explicit form:

$$m_i(t) = \sum_{\sigma_i(t),\sigma_{\partial i}(t-1)} p[\sigma_{\partial i}(t-1)]\sigma_i(t) \times \frac{e^{\beta\sigma_i(t)[\sum_{j\in\partial i} J_{ji}\sigma_j(t-1)+\theta_i(t)]}}{2\cosh\left[\beta\left(\sum_{j\in\partial i} J_{ji}\sigma_j(t-1)+\theta_i(t)\right)\right]}, \tag{11}$$

where $\sigma_{\partial i}$ is the collection of spins neighboring i with $c_{ji} \neq 0$, and $p[\sigma_{\partial i}(t-1)]$ is the corresponding joint probability distribution. In a fully asymmetric network, when an interaction coefficient J_{ji} in the above is nonzero, then the opposite J_{ij} is zero. Each of the spins $\sigma_j(t-1)$ on the right-hand side, therefore, does not depend directly on spin i on yet one time step before, i.e., on $\sigma_i(t-2)$. Furthermore, the distribution of each of the $\sigma_j(t-1)$ will in turn depend on distributions of other $\sigma_k(t-2)$, but the distribution of these $\sigma_k(t-2)$ does not depend on the $\sigma_j(t-1)$. If there are no short paths in the interaction graph between any pairs of spins σ_j on the right-hand side of (11) except through the cavity spin $\sigma_i(t)$, or if such paths are unimportant, then the spins $\sigma_j(t-1)$ will be independent in an asymmetric network, and the effective field $h_i(t) = \theta_i(t) + \sum_{j\in\partial i} J_{ji}\sigma_j(t-1)$ acting on $\sigma_i(t)$ will be the sum of independent random variables.

When the number of interacting spins is large, the distribution of $h_i(t)$ follows from the central limit theorem,

$$p[h_i(t)] = \frac{1}{\sqrt{2\pi V_i(t)}} \exp\left[-\frac{[h_i(t) - \langle h_i(t)\rangle]^2}{2V_i(t)} \right], \tag{12}$$

where $\langle h_i(t)\rangle = \theta_i(t) + \sum_{j\in\partial i} J_{ji}m_j(t-1)$ and $V_i(t) = \langle h_i(t)\rangle^2 - \langle h_i^2(t)\rangle$. We note that to arrive at this result, first the thermodynamic limit ($N \to \infty$) is taken at given connectivity

c [so that the terms $J_{ji}m_j(t-1)$ are independent], and then c is taken large (so that there are many of them). In general, $V_i(t)$ is defined as

$$V_i(t) = \sum_{j\in\partial i,k\in\partial i} J_{ji}J_{ki}[\langle\sigma_j(t-1)\sigma_k(t-1)\rangle - m_j(t-1)m_k(t-1)]. \quad (13)$$

With the additional assumption that the interaction coefficients J_{ji} are random, independent, evenly distributed, and small, the sum is dominated by the diagonal terms, i.e.,

$$V_i(t) = \sum_{j\in\partial i} J_{ji}^2\left[1-m_j^2(t-1)\right]. \quad (14)$$

This gives the "exact mean-field" theory of [30]:

$$m_i(t) = \int Dx\ \tanh\left[\beta\left(\theta_i(t)+\sum_j J_{ji}m_j(t-1) + x\sqrt{\sum_j J_{ji}^2[1-m_j^2(t-1)]}\right)\right] \quad (15)$$

with the Gaussian measure $Dx = \frac{dx}{\sqrt{2\pi}}e^{-\frac{x^2}{2}}$. Equation (15) can be iterated starting from some initial condition to get all magnetizations at any time, and is exact when the assumptions hold, i.e., when the network is fully asymmetric, when the cavity assumptions hold, when any spin is influenced by a large number of other spins, and when the interactions are random, independent, evenly distributed, and small.

To expand (15) in small interactions, we introduce $c_i(t) \equiv \sqrt{\sum_j J_{ji}^2[1-m_j^2(t-1)]}$ and take all these quantities of order ϵ. We have

$$\begin{aligned}&\tanh\{\beta[\langle h_i(t)\rangle + c_i(t)x]\}\\ &\quad= \tanh[\beta\langle h_i(t)\rangle] + xc_i(t)\beta\{1-\tanh^2[\beta\langle h_i(t)\rangle]\}\\ &\qquad -x^2c_i^2\beta^2\tanh[\beta\langle h_i(t)\rangle]\{1-\tanh^2[\beta\langle h_i(t)\rangle]\} + O(\epsilon^3),\end{aligned} \quad (16)$$

where every odd term in this expansion will give zero when integrated against a Gaussian measure. Therefore, we have

$$m_i(t) = \tanh[\beta\langle h_i(t)\rangle] - \beta^2\tanh[\beta\langle h_i(t)\rangle] \times\{1-\tanh^2[\beta\langle h_i(t)\rangle]\}c_i^2(t) + O(\epsilon^4). \quad (17)$$

We would like to write the right-hand side of (17) as $\tanh\{\beta[\langle h_i(t)\rangle + \Delta_i(t)]\} + O(\epsilon^4)$. A comparison shows that this is possible setting $\Delta_i(t) = \beta\tanh[\beta\langle h_i(t)\rangle]c_i^2(t)$. We therefore have to *fourth* order the following functional expression:

$$m_i(t) = \tanh\left(\beta\{\langle h_i(t)\rangle - \beta\tanh[\beta\langle h_i(t)\rangle]c_i^2(t)\}\right) + O(\epsilon^4). \quad (18)$$

To first order in ϵ, the solution is

$$m_i(t) = \tanh\left[\beta\left(\sum_{j\in\partial i}J_{ji}m_j(t-1)+\theta_i(t)\right)\right] + O(\epsilon^2), \quad (19)$$

which is the "dynamic naive mean field." Inserting this back in (18), we have the "dynamic TAP" of [28,29],

$$m_i(t) = \tanh\left[\beta\left(\sum_{j\in\partial i}J_{ji}m_j(t-1)+\theta_i(t)\right) - \beta^2m_i(t)\sum_{j\in\partial i}J_{ji}^2[1-m_j^2(t-1)]\right] + O(\epsilon^4). \quad (20)$$

The last term inside the tanh is of order ϵ^2 and a form analogous to the Onsager backreaction term; there is no third-order correction in ϵ in this theory.

B. The information geometry viewpoint

We will now derive the analogs of (19), (20), and a third-order term by following the approach of information geometry [3,18,37]. Let $\vec\sigma(0),\ldots,\vec\sigma(t)$ be the time history of a collection of spins. We assume that these spins have been generated by a kinetic Ising model with parallel updates and (possibly) time-dependent external fields. The joint probability of the history of all the spins is then

$$\begin{aligned}&P(\vec\sigma(0),\ldots,\vec\sigma(T)|\vec\theta(0),\ldots,\vec\theta(T),\{J_{ij}\})\\ &\quad= \prod_{t=1}^{T}\prod_i \exp(\sigma_i(t)h_i(t))/2\cosh(h_i(t)),\\ &h_i(t) = \theta_i(t) + \sum_j J_{ji}\sigma_j(t-1).\end{aligned} \quad (21)$$

In information geometry, the space of these model is considered as a manifold with coordinates being the (many) parameters $\vec\theta(0),\ldots,\vec\theta(T),\{J_{ij}\}$. A submanifold is the family of independent models,

$$\begin{aligned}&P^{\rm ind}(\vec\sigma(0),\ldots,\vec\sigma(T)|\vec\theta^{\rm ind}(0),\ldots,\vec\theta^{\rm ind}(T))\\ &\quad= \prod_{t=1}^{T}\prod_i \exp(\sigma_i(t)h_i(t))/2\cosh(h_i(t)),\\ &h_i(t) = \theta_i^{\rm ind}(t).\end{aligned} \quad (22)$$

A mean-field approximation is defined as the independent model with the same magnetizations as the full model [37]. For our case, it is easily seen that $m_i(t) = \tanh[\theta_i^{\rm ind}(t)]$ is the variational equation with respect to parameter $\theta_i^{\rm ind}(t)$ of the Kullback-Leibler divergence $D_{-1}[p|p^{\rm ind}] = \sum p\ln\frac{p}{p^{\rm ind}}$. Therefore, the mean-field approximation in information geometry can also be seen as the independent model with the least Kullback-Leibler divergence from the full model [3,18,37].

Following the approach of [18], we take the interaction parameters (J_{ij}) as small parameters (of order ϵ), and we assume that the differences $\Delta\theta_i(t) = \theta_i(t) - \theta_i^{\rm ind}(t)$ can be

expanded in ϵ:

$$\Delta\theta_i(t) = \epsilon\Delta_i^{(1)}(s) + \epsilon^2\Delta_i^{(2)}(s) + \cdots . \tag{23}$$

We can then write, in analogy with Eq. 3.2 of [18],

$$\begin{aligned} 0 = m_i(t) - m_i^{\text{ind}}(t) &= \epsilon \sum_{i,s} \left.\frac{\partial m_i(t)}{\partial\theta_i(s)}\right|_{\text{ind}} \Delta_i^{(1)}(s) \\ &+ \epsilon \sum_{j,k} \left.\frac{\partial m_i(t)}{\partial J_{kl}}\right|_{\text{ind}} J_{kl} + \epsilon^2 \sum_{i,s} \left.\frac{\partial m_i(t)}{\partial\theta_i(s)}\right|_{\text{ind}} \Delta_i^{(2)}(s) \\ &+ \frac{\epsilon^2}{2} \sum_{JK} \left.\frac{\partial^2 m_i(t)}{\partial\Theta_J\partial\Theta_K}\right|_{\text{ind}} \Delta^{(1)}\Theta_J\Delta^{(1)}\Theta_K + O(\epsilon^3). \end{aligned} \tag{24}$$

Here Θ_J stands for the set of all interacting couplings and external fields and J runs over relevant indices. The subscript indicates that all derivatives are evaluated at the independent model, and the left-hand side is zero because this is the variational equation. In the last term, the sum goes over all the parameters labeled J,K and the parameter increments are the first-order terms $\Delta_i^{(1)}(s)$ and J_{kl}; on third and higher orders, mixed terms of $\Delta_i^{(1)}(s)$ and $\Delta_i^{(2)}(s)$ will appear. A calculation presented in Appendix A gives the results

$$\Delta_i^{(1)}(t) = -\sum_j J_{ji} m_j(t-1), \tag{25}$$

$$\Delta_i^{(2)}(t) = m_i(t) \sum_k J_{ki}^2 \big[1 - m_k^2(t-1)\big], \tag{26}$$

$$\Delta_i^{(3)}(t) = -\sum_k \big[1 - m_k^2(t-1)\big] J_{ki} \Delta_k^{(2)}(t-1). \tag{27}$$

Equation (23) together with the variational equation can be rewritten as

$$\begin{aligned} &\tanh^{-1} m_i(t) \\ &\quad = \theta_i(t) - \epsilon\Delta_i^{(1)}(s) - \epsilon^2\Delta_i^{(2)}(s) - \epsilon^3\Delta_i^{(3)}(s) + O(\epsilon^4). \end{aligned} \tag{28}$$

It is seen that to ϵ this is "dynamic naive mean field" [compare (19)], to ϵ^2 this is "dynamic TAP" [compare (20)], and to ϵ^3 typically there is a nonzero term absent in (20). Such a higher-order difference between the exact mean-field theory for the asymmetric model and the field-theoretical approach of [28,29] was also pointed out in [30] (p. 4, in text below Eq. (7)).

IV. DYNAMIC CAVITY METHOD

The cavity method for equilibrium systems was introduced in [38,39] while the dynamic version was studied only recently [19–21]. In contrast to the equilibrium case, using only the cavity assumption does not in general provide us with an efficient algorithm in the dynamic case, but further assumptions are necessary. In this section, we derive the dynamic cavity method for the kinetic Ising problem, taking a more explicit route than in [20] and [21].

A. Cavity and BP on spin histories

We consider a number of spins evolving according to a dynamics such as (5), and we let X_i denote the whole history of spin i, $X_i = (\sigma_i(0),\sigma_i(1),\ldots,\sigma_T(0))$. The probability in (5) can then be alternatively interpreted as a joint probability of spin histories, $P(X_1,X_2,\ldots,X_N)$, and this probability can be represented by a graph where nodes i and j are connected if either J_{ij} or J_{ji} (or both) are nonzero. The corresponding product form is

$$\begin{aligned} &P(X_1,X_2,\ldots,X_N) \\ &\quad = \prod_i e^{\sum_s \theta_i(s)\sigma_i(s)} \prod_{ij} e^{\sum_s J_{ij}\sigma_i(s)\sigma_j(s+1)} \\ &\qquad \times \prod_i e^{-\sum_s \log 2\cosh[\theta_i(s)+\sum_j J_{ji}\sigma_j(s-1)]}, \end{aligned} \tag{29}$$

which is already normalized. Belief propagation is expected to work well if this graph is locally treelike, i.e., if all loops are long, and can be ignored [5]. In (29), this is never the case, even if the couplings are fully asymmetric, for the simple reason that if spins i and j drive spin k, then they are coupled both by the terms $\sigma_i(t)\sigma_k(t+1)$ and $\sigma_j(t)\sigma_k(t+1)$, and by the normalization $\log 2\cosh h_k(t+1)$. However, these couplings are of a rather peculiar type. To proceed, we introduce four different marginal probabilities. The first P_i is the marginal probability of spin history X_i. The second $P_{i+\partial i}$ is the marginal probability on the set of histories $\{X_i \bigcup X_{\partial i}\}$. The third $P_{\partial i}$ is the marginal on the set of histories $X_{\partial i}$. The fourth and last is $P^{(i)}$, a cavity distribution on $X_{\partial i}$. We take this as the marginal on $X_{\partial i}$ in a revised model in which both the spin history X_i as well as the normalization $\log 2\cosh h_i(t)$ have been eliminated. All four probabilities depend on external field parameters that are not necessarily the same. In particular, we will express $P_{\partial i}$ with one set of external fields and $P^{(i)}$ with another set of external fields. By definition, $P_{i+\partial i} = W(X_i|\,X_{\partial i})P_{\partial i}$. The peculiarity of the model is that the (normalized) conditional probability $W(X_i|\,X_{\partial i})$ is already explicitly included in (29). We can therefore compare

$$\begin{aligned} P_{\partial i}(\vec{X}_{\partial i}) = \frac{P_{i+\partial i}(X_i \bigcup X_{\partial i})}{W(X_i|X_{\partial i})} &\propto \prod_{j\in\partial i} e^{\sum_s \theta_j(s)\sigma_j(s)+\sum_{k\in\partial j}\sum_s J_{kj}\sigma_k(s)\sigma_j(s+1)-\sum_s \log 2\cosh[\theta_j(s)+\sum_k J_{kj}\sigma_k(s-1)]} \\ &\times \sum_{\vec{X}\setminus\{X_i\bigcup X_{\partial i}\}} \prod_{k\neq i,\partial i} \left(e^{\sum_s \theta_k(s)\sigma_k(s)} \prod_{l\in\partial k} e^{\sum_s J_{kl}\sigma_k(s)\sigma_l(s+1)} \prod_k e^{-\sum_s \log 2\cosh[\theta_k(s)+\sum_l J_{lk}\sigma_l(s-1)]} \right) \end{aligned} \tag{30}$$

to

$$\begin{aligned} P^{(i)}(X_{\partial i}) &\propto \prod_{j\in\partial i} e^{\sum_s \theta_j(s)\sigma_j(s)+\sum_{k\in\partial j,k\neq i}\sum_s J_{kj}\sigma_k(s)\sigma_j(s+1)-\sum_s \log 2\cosh[\theta_j(s)+\sum_{k\neq i} J_{kj}\sigma_k(s-1)]} \\ &\times \sum_{\vec{X}\setminus\{X_i\bigcup X_{\partial i}\}} \prod_{k\neq i,\partial i} \left(e^{\sum_s \theta_k(s)\sigma_k(s)} \prod_{l\in\partial k} e^{\sum_s J_{kl}\sigma_k(s)\sigma_l(s+1)} \prod_k e^{-\sum_s \log 2\cosh[\theta_k(s)+\sum_l J_{lk}\sigma_l(s-1)]} \right). \end{aligned} \tag{31}$$

This comparison shows that $P_{\partial i}$ with external fields $\theta_j(t)$ is the same as $P^{(i)}$ with *modified* external fields $\theta_j(t) + J_{ij}\sigma_i(t-1)$. Since $P_i(X_i) = \sum_{X_{\partial i}} W(X_i \mid X_{\partial i}) P_{\partial i}(X_{\partial i})$, we can therefore write the marginal probability P_i as

$$\begin{aligned} &P_i(X_i \mid \theta_i(0), \ldots, \theta_i(t), \cdot\,) \\ &\quad = \sum_{\sigma_{\partial i}(0)\cdots\sigma_{\partial i}(t-1)} P^{(i)}\big(X_{\partial i}(0) \mid \theta^{(i)}_{\partial i}(0), \ldots, \theta^{(i)}_{\partial i}(t), \cdot\,\big) \\ &\qquad \times \prod_{s=1}^{t} W_i[\sigma_i(s) \mid h_i(s)]\ p_i[\sigma_i(0)], \end{aligned} \tag{32}$$

where $\cdot$ indicates all the parameters (external fields and interactions) that are the same on the two sides of the equation, and

$$\theta^{(i)}_j(s) = \theta_j(s) + J_{ij}\sigma_i(s-1), \quad s = 0, \ldots, t \tag{33}$$

is the set of external fields that are modified.

The next step is to make the belief propagation assumption that the spin histories are taken independent in the cavity graph:

$$\begin{aligned} &P^{(i)}\big(X_{\partial i} \mid \theta^{(i)}_{\partial i}(0), \ldots, \theta^{(i)}_{\partial i}(t), \cdot\,\big) \\ &\quad = \prod_{j\in\partial i} \mu_{j\to i}\big(X_j \mid \theta^{(i)}_j(0), \ldots, \theta^{(i)}_j(t), \cdot\,\big). \end{aligned} \tag{34}$$

Here we used $\mu_{i\to j}$ to represent marginal probabilities of neighboring spins, as is standard in the BP literature.

We now consider the subgraph $T^{(i)}_j$ connected to one spin j in the cavity of i. In analogy to that presented above, we want to compare the marginal on the set of neighbors to spin j in $T^{(i)}_j$ to the cavity distribution on the same set of variables. As above, the first with one set of external fields is the same as the second with another set of external fields, and we therefore find the following recursion equations ("BP update equations"):

$$\begin{aligned} &\mu_{j\to i}\big(X_j \mid \theta^{(i)}_j(0), \ldots, \theta^{(i)}_j(t), \cdot_{T^{(i)}_j}\big) \\ &\quad = \sum_{X_{\partial j\setminus i}} \prod_{k\in\partial j\setminus i} \mu_{k\to j}\big(X_k \mid \theta^{(i),(j)}_k(0), \ldots, \theta^{(i),(j)}_k(t-1), \cdot_{T^{(i)}_j}\big) \\ &\qquad \times \prod_{s=1}^{t} w_j\big[\sigma_j(s) \,\big|\, h^{(i)}_j(s)\big]\ \ \mu_{j\to i}[\sigma_j(0)], \end{aligned} \tag{35}$$

where $\cdot_{T^{(i)}_j}$ indicates all the parameters (external fields and interactions) that are the same on the two sides of the equation, and

$$\theta^{(i),(j)}_k(s) = \theta^{(i)}_k(s) + J_{jk}\sigma_j(s-1), \quad s = 0, \ldots, t \tag{36}$$

is the set of external fields that are modified. Since in fact $\theta^{(i)}_k(s) = \theta_k(s)$ (spin k is not directly connected to i), we note that in (36) the upper index (i) can be dropped on both sides. The effective field on spin j in $T^{(i)}_j$ is

$$h^{(i)}_j(s) = \sum_{k\in\partial j\setminus i} J_{kj}\,\sigma_k(s-1) + \theta_j(s) \tag{37}$$

and $w_j[\sigma_j \mid h^{(i)}_j(s)]$ is the transition probability for the single spin j in the model on $T^{(i)}_j$.

The marginal probability over the history of one spin ("BP output equation") follows from (32) and (34) and is

$$\begin{aligned} &P_i(X_i \mid \theta_i(0), \ldots, \theta_i(t), \cdot\,) \\ &\quad = \sum_{X_{\partial i}} \prod_{k\in\partial i} \mu_{k\to i}\big(\sigma_k(0), \ldots, \sigma_k(t-1) \mid \theta^{(i)}_k(0), \ldots, \theta^{(i)}_k(t-1), \cdot\,\big) \\ &\qquad \times \prod_{s=1}^{t} W_i[\sigma_i(s) \mid h_i(s)]\ p_i[\sigma_i(0)]. \end{aligned} \tag{38}$$

Equations (35) and (38) are the dynamic cavity equations for our system. Both are large sets of equations connecting marginal distributions and cavity distributions between two probabilistic models with different parameters. In general, these equations are (as far as we know) only of conceptual value since on top of connecting different models, the right-hand side also involves on the order of $2^{T|\partial i|}$ operations. In BP, such an operation would have to be iterated (for all variables) a number of times to reach convergence: as T grows large, this becomes unfeasible for the same reason that ordinary BP does not work well if the state space of each variable is large.

We can define (and will later use) marginalizations of the messages down to one time (it is no restriction to take this time as the last time):

$$\begin{aligned} &\mu^t_{j\to i}\big[\sigma_j(t) \big| \theta^{(i)}_j(t)\big] \\ &\quad = \sum_{\sigma_j(0),\ldots,\sigma_j(t-1)} \mu_{j\to i}(\sigma_j(0), \ldots, \sigma_j(t) \mid \theta^{(i)}_j(0), \ldots, \theta^{(i)}_j(t)) \end{aligned} \tag{39}$$

but in general these quantities do not obey closed equations among themselves. An important exception are fully asymmetric networks, since there at most one of J_{ij} and J_{ji} is nonzero. We note that in (35) and (38), the probability distribution of spin i depends on the neighbors ∂i through the effective fields $h^{(i)}_j(s)$ and $h_i(s)$, but the messages sent from the neighbors to i also depend parametrically on the history of i through the modified external fields $\theta^{(i)}_k$. This backaction is absent for the fully asymmetric case where $\theta^{(i)}_k = \theta_k$ independent of spin i.

B. The projected dynamic BP

As discussed, the marginalization of dynamic BP over one time is not in general a Markov process. However, the long-time behavior of dynamics (stationary state) is often demanded in many cases. In this section, we explain an approximation scheme for computing marginal probabilities for one spin over one time in stationary state, a procedure called *one-time approximation* in [20] and *time factorization* in [21,22].

We start with the dynamic BP for the time histories of messages, i.e., Eq. (35), where on the right-hand side the time trajectory of messages sent from neighboring spins carries the information from the whole time history of those spins. We note that the full dynamics Eq. (5) is in fact Markov. This, and the need to introduce some approximation, motivates *the*

time-factorization ansatz, which we write for the terms on the right-hand side of Eq. (35):

$$\mu_{k\to j}(\sigma_k(0),\ldots,\sigma_k(t)\,|\,\cdot_{T_k^{(j)}}) = \prod_{s=0}^{t} \mu^s_{k\to j}\big[\sigma_k(s)\,|\,\cdot_{T_k^{(j)}}\big], \quad (40)$$

where $\cdot_{T_k^{(j)}}$ indicates the parameters of the model, the same on both sides. Obviously, when inserted into the right-hand side of (35), such a factorization is not preserved on the left-hand side. Since we deal with binary variables, we can introduce *time-factorized cavity biases* $u^{T_k^{(j)}}_{k\to j}(s)$, again written for the right-hand side of (35), which are defined by

$$\mu^s_{k\to j}\big[\sigma_k(s)\,|\,\cdot_{T_k^{(j)}}\big] = \frac{e^{\beta[\,u^{T_k^{(j)}}_{k\to j}(s)\,\sigma_k(s)]}}{2\cosh\left[\beta\left(u^{T_k^{(j)}}_{k\to j}(s)\right)\right]}. \quad (41)$$

A crucial observation is now that when the time-factorization ansatz has been made, the cavity biases at different external fields are simply related. We will need

$$u^{T_k^{(j)}}_{k\to j}(s) = u^{T_j^{(i)}}_{k\to j}(s) + J_{jk}\sigma_j(s-1), \quad s=0,\ldots,t, \quad (42)$$

which follows from the relation (36). Inserting (41) and (42) into (35) gives

$$\begin{aligned}
&\mu_{j\to i}(\sigma_j(0),\ldots,\sigma_j(t)|\,\cdot_{T_j^{(i)}}) \\
&= \sum_{\sigma_{\partial j\setminus i}(0),\ldots,\sigma_{\partial j\setminus i}(t-1)} \prod_{s=0}^{t}\prod_{k\in\partial j\setminus i} \\
&\quad\times \frac{e^{\beta\sigma_k(s)(\,u^{T_j^{(i)}}_{k\to j}(s)+J_{jk}\sigma_j(s-1))}}{2\cosh\left[\beta\left(u^{T_j^{(i)}}_{k\to j}(s)\,+J_{jk}\sigma_j(s-1)\right)\right]} \\
&\quad\times \prod_{s=1}^{t} w_j\big[\sigma_j(s)\,\big|\,h_j^{(i)}(s)\big]\mu_{j\to i}[\sigma_j(0)]. \quad (43)
\end{aligned}$$

This equation can be marginalized explicitly over the last time to give

$$\begin{aligned}
&\mu^t_{j\to i}[\sigma_j(t)|\,\cdot_{T_j^{(i)}}] \\
&= \sum_{\sigma_j(t-2),\sigma_{\partial j\setminus i}(t-1)} \prod_{k\in\partial j\setminus i} \\
&\quad\times \frac{e^{\beta\sigma_k(s)(u^{T_j^{(i)}}_{k\to j}(t-1)+J_{jk}\sigma_j(t-2))}}{2\cosh\left[\beta\left(u^{T_j^{(i)}}_{k\to j}(t-1)+J_{jk}\sigma_j(t-2)\right)\right]} \\
&\quad\times w_j[\sigma_j(t)|h_j^{(i)}(t)]\mu^{t-2}_{j\to i}[\sigma_j(t-2)|\,\cdot_{T_j^{(i)}}]. \quad (44)
\end{aligned}$$

The *projected dynamic cavity* is then to use (44) to compute the terms in a time factorization of the left-hand side of Eq. (35). Except for fully asymmetric models (with parallel updates), this approach is not appropriate for transients [22]. However, when the external fields θ_i are constant in time and when a stationary state has been reached, it may be acceptable to also take the messages independent in time. For one and the same set of parameter values, the fixed-point equations for the time-independent time-factorized cavity biases are then

$$\begin{aligned}
u^*_{j\to i} &= \frac{1}{2\beta}\sum_{\sigma_j}\sigma_j \log\left[\sum_{\sigma_{\partial j\setminus i},\sigma'_j} \frac{e^{\beta\sum_{k\in\partial j\setminus i}\sigma_k(u^*_{k\to j}+J_{jk}\sigma'_j)}}{2\cosh[\beta(u^*_{k\to j}+J_{jk}\sigma'_j)]}\right. \\
&\quad\left.\times \frac{e^{\beta\,h_j^{(i)}\sigma_j}}{2\cosh(\beta\,h_j^{(i)})}\;\frac{e^{\beta\sigma'_j u^*_{j\to i}}}{2\cosh(\beta u^*_{j\to i})}\right], \\
h_j^{(i)} &= \sum_{k\in\partial j\setminus i} J_{kj}\,\sigma_k + \theta_j. \quad (45)
\end{aligned}$$

Equation (45) is an ordinary BP solved by iteration, where the right-hand side is computed from $u^{(t-1)}_{k\to j}$ at iteration time $t-1$, giving the left-hand side $u^{(t)}_{j\to i}$ at iteration time t. The spin σ_j summed over is then conceptually at time t, the spins σ_k at time $t-1$, and the last spin σ'_j at time $t-2$, all these in the iteration time.

Using the iteration time as a proxy for real time, we note that in a transient, we can compute the time evolution of

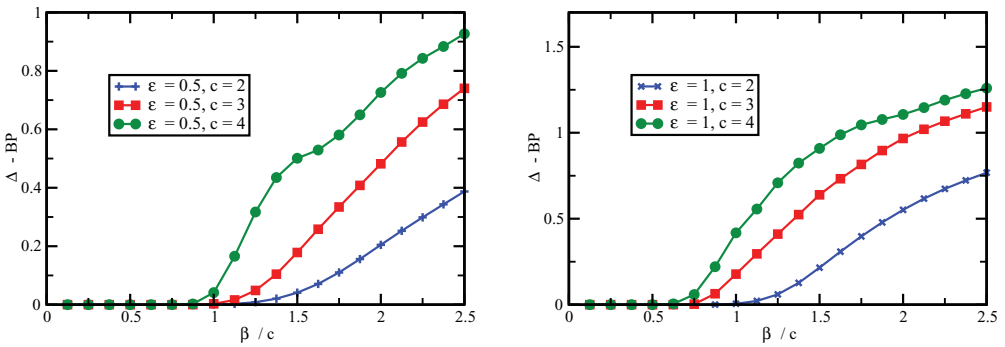

FIG. 1. (Color online) Squared deviation of spin averages between successive update $\Delta(t) = 1/N\sum_{i=1}^{N}[m_i(t)-m_i(t-1)]^2$ at the stationary limit for different values of average connectivity c. Mean magnetizations are calculated by the projected dynamic cavity method, i.e., Eq. (46). Left panel: partially asymmetric networks with $\epsilon = 0.5$. Right panel: symmetric network $\epsilon = 1$. The results are averaged over BP initial conditions (10 experiences). System size is 1000 and external fields are set to zero.

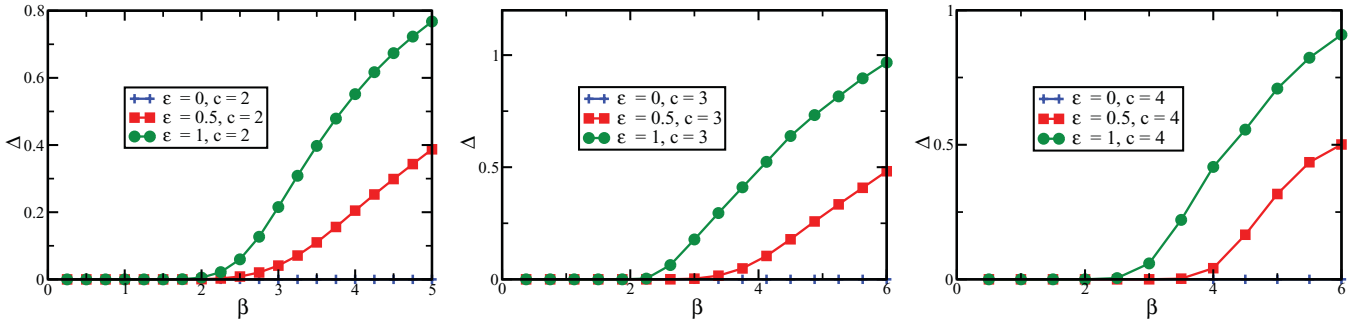

FIG. 2. (Color online) Effect of asymmetry ($\epsilon = 0, 0.5, 1$) in squared deviation of spin averages between successive update $\Delta(t) = 1/N \sum_{i=1}^{N} [m_i(t) - m_i(t-1)]^2$, obtained by projected dynamic BP Eq. (46), at the stationary limit for average connectivity $c = 2$ (left panel), $c = 3$ (middle panel), and $c = 4$ (right panel). The results are averaged over BP initial conditions (10 experiences). System size is 1000 and external fields are set to zero.

magnetization that would follow from (41) and (37),

$$m_i(t) = \sum_{\sigma_{\partial i\setminus j}(t-1),\sigma_i(t-2)} \frac{e^{\beta \sum_{k\in\partial i\setminus j}[u_{k\to i}(t-1)+J_{ik}\sigma_i(t-2)]\sigma_k(t-1)}}{\prod_{k\in\partial i\setminus j} 2\cosh\{\beta\,[u_{k\to i}(t-1) + J_{ik}\sigma_i(t-2)]\}} \tanh\left[\beta\left(\sum_{j\in\partial i} J_{ji}\,\sigma_j(t-1) + \theta_i\right)\right] \times \frac{e^{\beta u_{i\to j}(t-2)\sigma_i(t-2)}}{2\cosh[\beta u_{i\to j}(t-2)]}. \tag{46}$$

This is not expected to be accurate unless we are already in a stationary state. We use it below in Sec. V as a proxy to monitor if the system is in a stationary state.

V. RESULTS

In this section, we investigate the performance of the dynamic cavity method in computing stationary states of diluted spin glass in parallel update, and we compare to MCMC (Glauber dynamics) and to dynamic mean-field and dynamic TAP as defined in Sec. III. The convergence of the projected dynamic cavity (the dynamic cavity in the time-factorized approximation) is monitored by comparing the magnetization computed from (46) at successive times for different parameter values of the model, and these predictions are then compared to dynamic mean-field and dynamic TAP and MCMC.

A. Convergence of dynamic BP

In order to detect where dynamic BP reaches a stationary state, we compare single magnetization in two successive time steps as

$$\Delta(t) = 1/N \sum_{i=1}^{N} [m_i(t) - m_i(t-1)]^2. \tag{47}$$

Whenever this deviation vanishes, dynamic BP must have converged to a stationary state. Figure 1 shows the results for various connectivity parameters in symmetric and partially symmetric networks. In high temperature, we observe convergence toward a fixed point, whereas in low temperature, BP does not reach a stationary state. Roughly speaking, dynamic BP stops converging at a value $\beta_{cr}(c)$, which depends on the average connectivity.

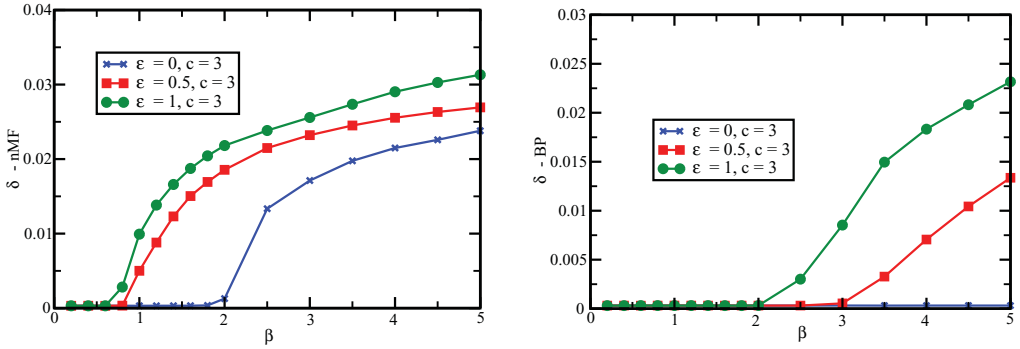

FIG. 3. (Color online) Mean-square error $\delta(t) = 1/N \sum_{i=1}^{N} [m_i^{\text{predicted}}(t) - m_i^{\text{empirical}}(t)]^2$ of the two approximation methods (dynamic mean field and dynamic cavity) with respect to the empirical data (Glauber dynamics). Left panel: dynamic mean field Eq. (19) for networks with different asymmetric parameter ($\epsilon = 0, 0.5, 1$) and fixed average connectivity $c = 3$. Right panel: the corresponding results obtained by the projected dynamic cavity method Eq. (46) For small β, i.e., high temperature, they are in agreement with numerical simulations. In low β, however, dynamic BP outperforms dynamic mean field.

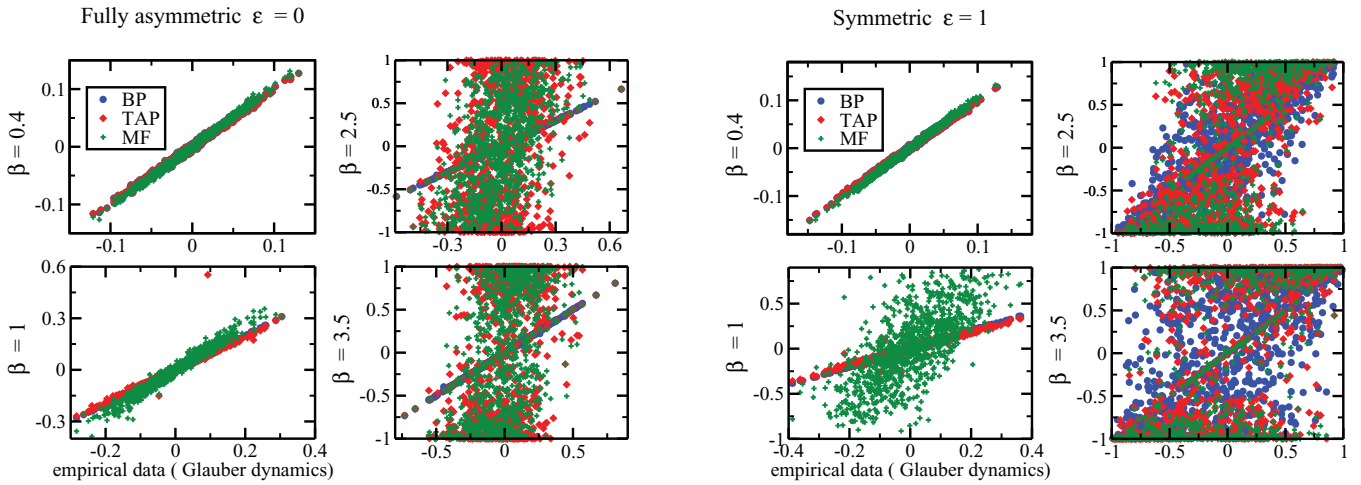

FIG. 4. (Color online) Scatter plot of local magnetizations for dilute asymmetric networks for four different temperature $\beta = 0.4, 1, 2.5, 3.5$ and a fixed average connectivity $c = 3$. Local magnetizations are obtained by dynamic mean field Eq. (19) (green), dynamic TAP Eq. (20) (red), and projected dynamic BP Eq. (46) (blue). Left panels show the scatter plots in fully asymmetric networks ($\epsilon = 0$), where the projected dynamic BP provides exact results; right panels are scatter plots in fully symmetric networks ($\epsilon = 1$). In high temperature, all three methods agree with numerical simulations. In low temperature, BP starts to outperform naive mean field and TAP.

In Fig. 2, the convergence of dynamic BP is plotted to show the effect of asymmetry. In this case, it is simply that for very asymmetric graphs, BP converges in a very wide region, presumably for arbitrarily large values of β if the network grows large enough, and, in general, the more asymmetric the network, the better the convergence.

B. Performance of dynamic BP

Figure 3 shows a comparison between the dynamic cavity method and the dynamic mean-field method for total magnetization in spin glass systems with different asymmetric parameters. The results are obtained in the presence of small external fields $\theta = 0.001$. The dynamic cavity method shows a strong agreement with numerical simulations of Glauber-type dynamics when it converges to a stationary state. The dynamic mean-field method, however, starts to deviate from numerical simulations already in small β, indicating that it is less accurate compared to the dynamic cavity method.

In order to observe the comparison in more detail, we show also the scatter plot of spin-by-spin magnetization in Fig. 4. The dynamic cavity method predicts perfectly local magnetizations for fully asymmetric networks and agrees quite well with numerical simulations in high temperature for the fully symmetric network, whereas naive mean field and TAP start to deviate already at moderate temperatures.

VI. CONCLUSION

Message-passing methods have become an important topic on the borderline between equilibrium statistical physics and information theory. In the present paper, we have studied an extension of message-passing to nonequilibrium Ising spin systems. In contrast to the equilibrium case, the cavity method is not immediately useful to describe the dynamics, even if the topology is suitable, because the messages depend on whole spin time histories. The time-factorization assumption, as discussed here and in [20–22] (or some other simplifying assumption), is necessary to reduce the complexity, but when so doing, one is generally restricted to stationary states.

We have studied the dynamic cavity in the time-factorized assumption for stationary states and outlined its convergence region in parameter strength (β), connectivity (c), and asymmetry (ϵ). In analogy with generally known facts about BP, it can be argued that when the dynamic cavity converges, it should typically be a good approximation; the region of convergence is therefore a useful proxy for accuracy. Expanding on the first results presented in [21], we show that the convergence region in β *increases* with the connectivity. We also find that the convergence region *increases* with asymmetry for several values of connectivity, and that it converges for any interaction strength for fully asymmetric networks (as expected). For networks of moderate size, we have directly compared the dynamic cavity and the dynamic mean field to direct simulation. For several values of asymmetry and connectivity, we find that their convergence regions are very similar, if not identical, but when both methods converge, then the dynamic cavity method is considerably more accurate except in the low-β limit, where their performance is about the same. We have hence shown that the dynamic cavity can be a useful new approximation to the dynamics of nonequilibrium spin systems—and any system that can be fruitfully modeled by such methods.

On the analytical side, we have discussed the special status of fully asymmetric models, for which the cavity approach is in some sense exact. We have also rederived the "dynamic TAP" equation of Hertz and Roudi [28,29] using a straightforward approach borrowed from Kappen and Spanjers' treatment of the stationary state [18], clarifying that this approach is based on minimizing the distance, in the sense of information geometry, to the subfamily of independent (but time-changing) models. Whether such a perturbative argument can be extended to small deviations from, e.g., fully asymmetric models remains to be seen.

ACKNOWLEDGMENTS

We thank Marc Mézard for important remarks, and Mikko Alava, Yoshiyuki Kabashima, Pekka Orponen, and Toshiyuki Tanaka for discussions. The work was supported by the Academy of Finland as part of its Finland Distinguished Professor program, project 129024/Aurell.

APPENDIX A: THE INFORMATION GEOMETRY CALCULATION TO SECOND ORDER

The following calculations are completely parallel to those in Appendix 1 of [18] and start from

$$\left.\frac{\partial m_i(t)}{\partial \theta_j(s)}\right|_{\text{ind}} = \delta_{s,t}\delta_{ij}\big(1-m_i^2(t)\big), \tag{A1}$$

$$\left.\frac{\partial m_i(t)}{\partial J_{jk}}\right|_{\text{ind}} = \delta_{ik}\big(1-m_i^2(t)\big)m_j(t-1), \tag{A2}$$

$$\left.\frac{\partial^2 m_i(t)}{\partial\theta_j(s)\partial\theta_k(s')}\right|_{\text{ind}} = -2m_i(t)\big[1-m_i^2(t)\big]\delta_{ij}\delta_{ik}\delta_{s,t}\delta_{s',t}, \tag{A3}$$

$$\left.\frac{\partial^2 m_i(t)}{\partial J_{jk}\partial\theta_l(s)}\right|_{\text{ind}} = -2m_i(t)\big[1-m_i^2(t)\big]m_j(t-1)\delta_{ik}\delta_{il}\delta_{s,t} + \big[1-m_i^2(t)\big]\big[1-m_j^2(t-1)\big]\delta_{ik}\delta_{kl}\delta_{s,t-1}, \tag{A4}$$

$$\begin{aligned}\left.\frac{\partial^2 m_i(t)}{\partial J_{jk}\partial J_{lm}}\right|_{\text{ind}} &= \delta_{ik}\big[1-m_i^2(t)\big]\big[1-m_j^2(t-1)\big]\delta_{lk}m_l(t-2) \\ &\quad + (jk)\leftrightarrow(lm) - 2m_i(t)\delta_{ik}\big(1-m_i^2(t)\big)\delta_{im} \\ &\quad \times\big(m_k(t-1)m_m(t-1)+\delta_{km}\big(1-m_k^2(t-1)\big)\big).\end{aligned} \tag{A5}$$

To first order in ϵ, (24) hence gives

$$\sum_{s,j}\delta_{s,t}\delta_{ij}\big(1-m_i^2(t)\big)\Delta_j^{(1)}(s) + \sum_{jk}\delta_{ij}\big(1-m_i^2(t)\big)m_k(t-1)J_{jk} = 0, \tag{A6}$$

which is simply

$$A_i^{(1)}(t) \equiv \Delta_i^{(1)}(t) + \sum_j J_{ji}m_j(t-1) = 0. \tag{A7}$$

This is the same as the "dynamic naive mean field,"

$$\tanh^{-1}[m_i(t)] = \theta_i(t) + \sum_k J_{ki}m_k(t-1) + O(\epsilon^2). \tag{A8}$$

The terms arising from second-order derivatives and first-order increments can be grouped together as

$$\big[1-m_i^2(t)\big]\left(-m_i(t)\big(A_i^{(1)}\big)^2(t) - \sum_j\big[1-m_j^2(t-1)\big] \times J_{ji}A_j^{(1)}(t-1) - m_i(t)\sum_k J_{ki}^2\big[1-m_k^2(t-1)\big]\right), \tag{A9}$$

which together with the first-order conditions (A7) and the term from the first-order derivative and second-order increment $[1-m_i^2(t)]\Delta_i^{(2)}(t)$ gives

$$\Delta_i^{(2)}(t) = m_i(t)\sum_k J_{ki}^2\big[1-m_k^2(t-1)\big]. \tag{A10}$$

This is the same as "dynamic TAP," compare (20) above,

$$\tanh^{-1}[m_i(t)] = \theta_i(t) + \sum_k J_{ki}m_k(t-1) - m_i(t)\sum_k J_{ki}^2m_k^2(t-1) + O(\epsilon^3). \tag{A11}$$

APPENDIX B: THE INFORMATION GEOMETRY CALCULATION TO THIRD ORDER

Third-order contributions consist partly of terms involving lower than third-order derivatives and higher than first-order increments. The calculations of these use the same elements as above and are

$$\sum_{j,s}\left.\frac{\partial m_i(t)}{\partial\theta_j(s)}\right|_{\text{ind}}\Delta_j^{(3)}(s) = \big[1-m_i^2(t)\big]\Delta_i^{(3)}(t), \tag{B1}$$

$$\sum_{j,s,k,s'}\left.\frac{\partial^2 m_i(t)}{\partial\theta_j(s)\partial\theta_k(s')}\right|_{\text{ind}}\Delta_j^{(2)}(s)\Delta_k^{(1)}(s') = -2m_i(t)\big[1-m_i^2(t)\big]\Delta_i^{(2)}(t)\Delta_i^{(1)}(t), \tag{B2}$$

$$\sum_{j,k,l,s}\left.\frac{\partial^2 m_i(t)}{\partial J_{jk}\partial\theta_l(s)}\right|_{\text{ind}}J_{jk}\Delta_l^{(2)}(s) = -2m_i(t)\big[1-m_i^2(t)\big]\sum_j m_j(t-1)J_{ji}\Delta_i^{(2)}(t) + \big[1-m_i^2(t)\big]\sum_k\big[1-m_k^2(t-1)\big]J_{ki}\Delta_k^{(2)}(t-1), \tag{B3}$$

where two terms can be combined to

$$-2m_i(t)\big[1-m_i^2(t)\big]\Delta_i^{(2)}(t)\left(\Delta_i^{(1)}(t)+\sum_k J_{ki}m_k(t-1)\right) = 0. \tag{B4}$$

The remainder is

$$\big[1-m_i^2(t)\big]\left(\Delta_i^{(3)}(t)+\sum_k\big[1-m_k^2(t-1)\big]J_{ki}\Delta_k^{(2)}(t-1)\right) \quad \text{(lower-order terms)}. \tag{B5}$$

To proceed with the terms from third-order derivatives and first-order increments, it is useful to introduce the streamlined notation,

$$m_i = m_i(t), \quad m_i' = m_i(t-1), \quad m_i'' = m_i(t-2), \quad \text{etc.} \tag{B6}$$

and similar for all other quantities. It is also useful to note that though the derivatives act on the complete expression involving both probability density P and the tanh , they partially obey a chain rule when taken to act on the magnetizations alone:

(i) A derivative with respect to an external field $\theta_j(s)$ functions as an ordinary derivative and obeys a chain rule.

(ii) A derivative with respect to an interaction coefficient J_{kl} acting on a once or more than once primed quantity, such as m_i' and m_i'', functions as an ordinary derivative and obeys the chain rule.

(iii) A derivative with respect to an interaction coefficient J_{kl} acting on an unprimed quantity such as m_i must be treated separately, since this derivative will include a term taken on the tanh, which in turn will give a higher-order correlation.

These rules allow us to continue from what has already been computed and write

$$\left.\frac{\partial m_i}{\partial\theta_j(s)}\right|_{\text{ind}} = \left(1-m_i^2\right)\delta_{ij}\delta_{st}, \quad \left.\frac{\partial^2 m_i}{\partial\theta_j(s)\partial\theta_k(s')}\right|_{\text{ind}} = -2m_i\left(1-m_i^2\right)\delta_{ij}\delta_{st}\delta_{ik}\delta_{s't},$$
$$\left.\frac{\partial^3 m_i}{\partial\theta_j(s)\partial\theta_k(s')\partial\theta_l(s'')}\right|_{\text{ind}} = 2\left(1-m_i^2\right)\left(3m_i^2-1\right)\delta_{ij}\delta_{st}\delta_{ik}\delta_{s't}\delta_{il}\delta_{s''t},$$
$$\vdots$$

For the mixed terms, we have similarly

$$\left.\frac{\partial m_i}{\partial J_{jk}}\right|_{\text{ind}} = \left(1-m_i^2\right)\delta_{ik}m_j', \quad \left.\frac{\partial^2 m_i}{\partial J_{jk}\partial\theta_l(s)\partial}\right|_{\text{ind}} = -2m_i\left(1-m_i^2\right)\delta_{il}\delta_{s,t}\delta_{ik}m_j' + \left(1-m_i^2\right)\delta_{ik}(1-(m_j')^2)\delta_{jl}\delta_{s,t-1},$$
$$\left.\frac{\partial^3 m_i}{\partial J_{jk}\partial\theta_l(s)\partial\theta_{l'}(s')}\right|_{\text{ind}} = 2\left(1-m_i^2\right)\left(3m_i^2-1\right)\delta_{il'}\delta_{s',t}\delta_{il}\delta_{s,t}\delta_{ik}m_j' - 2m_i\left(1-m_i^2\right)\delta_{il}\delta_{s,t}\delta_{ik}(1-(m_j')^2)\delta_{l'j}\delta_{s',t-1}$$
$$- 2m_i\left(1-m_i^2\right)\delta_{il'}\delta_{s',t}\delta_{ik}\left(1-(m_j')^2\right)\delta_{jl}\delta_{s,t-1} + (1-m_i^2)\delta_{ik}(-2m_j')[1-(m_j')^2]\delta_{jl}\delta_{s,t-1}\delta_{jl'}\delta_{s',t-1}$$
$$\vdots$$

and

$$\left.\frac{\partial^2 m_i}{\partial J_{jk}\partial J_{lm}}\right|_{\text{ind}} = \delta_{ik}\left(1-m_i^2\right)[1-(m_j')^2]\delta_{lk}m_l'' + (jk)\leftrightarrow(lm) - 2m_i\left(1-m_i^2\right)\delta_{ik}\delta_{im}(m_k'm_m' + \chi_{km}'),$$
$$\left.\frac{\partial^3 m_i}{\partial J_{jk}\partial J_{lm}\partial\theta_n(s)}\right|_{\text{ind}} = \delta_{ik}\big(-2m_i\left(1-m_i^2\right)\delta_{in}\delta_{s,t}(1-(m_j')^2)\delta_{lk}m_l''\big) + \delta_{ik}\left(1-m_i^2\right)\{-2m_j'[1-(m_j')^2]\delta_{jn}\delta_{s,t-1}\delta_{lk}m_l''\}$$
$$+\delta_{ik}\left(1-m_i^2\right)[1-(m_j')^2]\delta_{lk}(1-(m_l'')^2)\delta_{ln}\delta_{s,t-2} + (jk)\leftrightarrow(lm)$$
$$+2\left(1-m_i^2\right)(3m_i-1)\delta_{in}\delta_{s,t}\delta_{ik}\delta_{im}\langle\sigma_k(t-1)\sigma_m(t-1)\rangle - 2m_i\left(1-m_i^2\right)\delta_{ik}\delta_{im}(1-(m_k')^2)\delta_{kn}\delta_{s,t-1}m_m'$$
$$-2m_i\left(1-m_i^2\right)\delta_{ik}\delta_{im}m_k'[1-(m_m')^2]\delta_{mn}\delta_{s,t-1} - 2m_i\left(1-m_i^2\right)\delta_{ik}\delta_{im}\frac{\partial\chi_{km}'}{\partial\theta_n(s)}$$
$$\vdots$$

where we use the correlation function $\chi_{km} = \langle\sigma_k(t)\sigma_m(t)\rangle - m_km_m$. Its partial derivative with respect to an external field is always zero, and the last term in the above equations therefore vanishes. The more cumbersome term is three derivatives with respect to interaction coefficients, which we can start from

$$\left.\frac{\partial^3 m_i}{\partial_{pq}\partial J_{jk}\partial J_{lm}}\right|_{\text{ind}} = \frac{\partial}{\partial J_{pq}}\left[\begin{array}{l}\sum_\sigma \frac{\partial^2 P(\sigma)}{\partial J_{jk}\partial J_{lm}}\tanh(\cdot) + \sum_\sigma \frac{\partial P(\sigma)}{\partial J_{jk}}[1-\tanh^2(\cdot)]\delta_{im}\sigma_l(t-1) + (jk)\leftrightarrow(lm)\\ \times\sum_\sigma P(\sigma)[-2\tanh(\cdot)][1-\tanh^2(\cdot)]\delta_{im}\sigma_l(t-1)\delta_{ik}\sigma_j(t-1)\end{array}\right]. \tag{B7}$$

Applying ∂J_{pq} gives (at least conceptually) eight terms. The term from acting on $\frac{\partial^2 P(\sigma)}{\partial J_{jk}\partial J_{lm}}$ vanishes. The term from acting on $\tanh(\cdot)$ in the first line gives a second derivative with respect to interaction coefficients of a magnetization. The terms from the second and the third line give combinations involving either second derivatives of a magnetization or first derivatives of a correlation function. The terms from the last line are a third-order correlation function and further first derivatives of second-order correlation functions.

Taking all together, we can sum the contributions to

$$\begin{aligned}\text{Third order} = {} & \frac{1}{6}2\left(1-m_i^2\right)\left(3m_i^2-1\right)\left[A_i^{(1)}(t)\right]^3 + 2m_i\left(1-m_i^2\right)\Delta_i^{(1)}(t)\sum_l[1-(m_l')^2]J_{li}A_l^{(1)}(t-1) - \left(1-m_i^2\right)\sum_l J_{li}\left[A_l^{(1)}(t)\right]^2 \\ & + \frac{1}{2}2\left(1-m_i^2\right)\left(3m_i^2-1\right)A_i^{(1)}(t)\sum_{lm}J_{il}J_{im}\chi_{lm} - 2m_i\left(1-m_i^2\right)\sum_{ln}J_{li}[1-(m_l')^2]A_l^{(1)}(t-1)J_{ni}m_n' \\ & + \left(1-m_i^2\right)\sum_{ml}J_{mi}J_{lm}[1-(m_m')^2][1-(m_l'')^2]A_l^{(1)}(t-2) + (m)\leftrightarrow(l) - m_i\left(1-m_i^2\right)\sum_{ln,js}J_{li}J_{ni} \\ & \times\left(\frac{\partial\chi_{ln}(t-1)}{\partial\theta_j(s)}\right)\Delta_j^{(1)}(s) - \frac{1}{3}m_i\left(1-m_i^2\right)\sum_{ln,js}J_{li}J_{ni}\left(\frac{\partial\chi_{ln}(t-1)}{\partial J_{pq}}\right)J_{pq} + \text{circ. perm.} \\ & + \frac{1}{3}\left(1-m_i^2\right)\left(3m_i^2-1\right)\sum_{lnq}J_{li}J_{ni}J_{qi}\chi'_{lnq}, \end{aligned} \tag{B8}$$

where in the last line we have used $\chi_{lnq} = \langle[\sigma_l(t)-m_l][\sigma_n(t)-m_n][\sigma_q(t)-m_q]\rangle$. All the terms in the above containing the first-order terms $A^{(1)}$ vanish, the partial derivative terms of the second-order correlation function with respect to external field vanish, and the last line is at least smaller than ϵ^3. The sole remaining terms hence come from the partial derivatives of second-order correlation functions with respect to interaction parameters. These are model-dependent, and are evaluated to nonzero for the *sequential update* rule in [18]. For the *parallel update* rule that we look at here, however, they are zero. The collection of terms (B8), therefore, evaluates to zero.

[1] D. Thouless, P. Anderson, and R. Palmer, Philos. Mag. **35**, 593 (1977).

[2] G. Parisi, *Statistical Field Theory* (Addison-Wesley, Reading, MA, 1988).

[3] T. Tanaka, Neural Comput. **12**, 1951 (2000).

[4] J. S. Yedidia, W. T. Freeman, and Y. Weiss, *Understanding Belief Propagation and its Generalizations in Exploring Artificial Intelligence in the New Millennium* (Morgan Kaufmann, San Francisco, CA, 2003); in *Advances in Neural Information Processing Systems* 13 (MIT Press, Cambridge, MA, 2000), pp. 689–695.

[5] M. Mézard and A. Montanari, *Information, Physics and Computation* (Oxford University Press, 2009).

[6] J. Pearl, *Probabilistic Reasoning in Intelligent Systems: Networksg of Plausible Inference* (Morgan Kaufmann, San Francisco, 1988).

[7] J. Pearl, *Causality: Models, Reasoning, and Inference* (Cambridge University Press, 2000).

[8] M. Opper and O. Winther, Phys. Rev. E **64**, 056131 (2001).

[9] F. R. Kschischang, B. J. Frey, and H.-A. Loeliger, IEEE Trans. Inf. Theory **47**, 498 (1998).

[10] U. Frisch, *Turbulence* (Cambridge University Press, Cambridge, UK, 1995).

[11] N. van Kampen, *Stochastic Processes in Physics and Chemistry* (Elsevier, Amsterdam, 2007).

[12] J. J. Hopfield, Proc. Natl. Acad. Sci. (USA) **79**, 2554 (1982).

[13] R. A. Blythe and A. J. McKane, J. Stat. Mech.: Theor. Exp. (2007) P07018.

[14] B. Derrida, E. Gardner, and A. Zippelius, Europhys. Lett. **4**, 167 (1987).

[15] J. Hertz, G. Grinstein, and S. A. Solla, in *Neural Networks for Computing*, AIP Conf. Proc. No. 151, edited by J. Denker (AIP, New York, 1986).

[16] J. Hertz, G. Grinstein, and S. A. Solla, in *Heidelberg Conference on Glassy Dynamics and Optimization*, edited by I. Morgenstern and J. L. van Hemmen (Springer-Verlag, Berlin, 1987).

[17] A. Crisanti and H. Sompolinsky, Phys. Rev. A **37**, 4865 (1988).

[18] H. J. Kappen and J. J. Spanjers, Phys. Rev. E **61**, 5658 (2000).

[19] Y. Kanoria and A. Montanari, Ann. Appl. Prob. **21**, 1694 (2011).

[20] I. Neri and D. Bollé, J. Stat. Mech. (2009) P08009.

[21] E. Aurell and H. Mahmoudi, J. Stat. Mech. (2011) P04014.

[22] E. Aurell and H. Mahmoudi, Commun. Theor. Phys. **56**, 157 (2011).

[23] H. Sompolinsky and A. Zippelius, Phys. Rev. B **25**, 6860 (1982).

[24] A. Crisanti and H. Sompolinsky, Phys. Rev. A **36**, 4922 (1987).

[25] A. C. C. Coolen, S. N. Laughton, and D. Sherrington, Phys. Rev. B **53**, 8184 (1996).

[26] H. J. Sommers, Phys. Rev. Lett. **58**, 1268 (1987).

[27] J. P. L. Hatchett, B. Wemmenhove, I. P. Castillo, T. Nikoletopoulos, N. S. Skantzos, and A. C. C. Coolen, J. Phys. A **37**, 6201 (2004).

[28] Y. Roudi and J. Hertz, Phys. Rev. Lett. **106**, 048702 (2011).

[29] Y. Roudi and J. Hertz, J. Stat. Mech. (2011) P03031.

[30] M. Mézard and J. Sakellariou, J. Stat. Mech.: Theor. Exp. (2011) L07001.

[31] D. Sherrington and S. Kirkpatrick, Phys. Rev. Lett. **35**, 1792 (1975).

[32] A. Kholodenko, J. Stat. Phys. **58**, 355 (1990).

[33] T. Plefka, J. Phys. A **15**, 1971 (1982).

[34] J. Sakellariou, Y. Roudi, M. Mezard, and J. Hertz, e-print arXiv:1106.0452.

[35] U. Marconi, A. Puglisi, L. Rondoni, and A. Vulpiani, Phys. Rep. **461**, 111 (2008).

[36] J. Hertz, Y. Roudi, and J. Tyrcha, e-print arXiv:1106.1752.

[37] S. Amari, S. Ikeda, and H. Shimokawa, in *Information Geometry and Mean Field Approximation: The Alpha-projection Approach* (MIT Press, Cambridge, MA, 2001), pp. 241–257.

[38] M. Mezard, G. Parisi, and M. Virasoro, *Spin Glass Theory and Beyond* (World Scientific, Singapore, 1987).

[39] M. Mézard and G. Parisi, Eur. Phys. J. B **20**, 217 (2001).